Applied Surface Science 331 (2015) 66–71

Contents lists available at ScienceDirect

Applied Surface Science

journal homepage: www.elsevier.com/locate/apsusc

Amorphous self-lubricant MoS_2-C sputtered coating with high hardness

Lei Gu[a,b], Peiling Ke[b,*], Yousheng Zou[a,*], Xiaowei Li[b], Aiying Wang[b]

[a] School of Materials Science and Engineering, Institute of Optoelectronics & Nanomaterials, Nanjing University of Science and Technology, Nanjing, Jiangsu 210094, China

[b] Key Laboratory of Marine Materials and Related Technologies, Zhejiang Key laboratory of Marine Materials and Protective Technologies, Ningbo Institute of Materials Technology and Engineering, Chinese Academy of Sciences, Ningbo 315201, China

ARTICLE INFO

Article history:
Received 10 September 2014
Received in revised form
15 December 2014
Accepted 8 January 2015
Available online 16 January 2015

Keywords:
MoS_2
Carbon
Ti interlayer
Amorphous structure
Mechanical properties

ABSTRACT

MoS_2-C coatings with various carbon contents were deposited by direct current magnetron sputtering. Carbon concentration (from 40.9 at.% to 73.1 at.%) within the coatings was controlled by varying the number of MoS_2 plates bonded to the carbon targets. Ti interlayer fabricated by a hybrid high power impulse magnetron sputtering was used to obtain excellent adhesion. By sputtering the composite target, the deposited coatings exhibited a typical amorphous structure feature which contributed to the high hardness of the coatings. Meanwhile, the friction coefficient of the composite coating was lower than 0.1 in the ambient air and exhibited high wear resistance. Furthermore, the composite coatings exhibited an increasing hardness (from 7.0 to 10.8 GPa) with increasing carbon content.

1. Introduction

Transition metal dichalcogendies (sulfides, selenides or tellurides of molybdenum, tungsten and niobium) as solid lubricant coatings exhibit excellent self-lubricant properties in vacuum and dry air environment [1,2]. Among these transition metal dichalcogendies, sputtered MoS_2 coating has been widely used in the space field due to its ultra-low friction coefficient and high wear resistance in high vacuum environment [3,4]. In spite of its mature application in aerospace industry, pure MoS_2 coatings performs poorly in humid air environment, which is attributed to its loose structure, low hardness and high chemical activity to oxygen [5,6]. To improve tribological performance of MoS_2 coatings in ambient air, compositing MoS_2 with metal components (including Ti, Ag, W) has been a most popular method. Among these metals, Ti doped MoS_2 coatings have acquired successful commercial application. However, doping Ti does not contribute to low friction in humid environment [7–9].

Therefore, MoS_2 compositing with nonmetallic elements (C, N included) is gaining increasing attention, due to its low friction under humid air environment [10,11]. The concept is that MoS_2 as lubricant is distributed within hard carbon films and thus carbon matrix can protect MoS_2 from oxidation and improved mechanical properties of the coatings. Voevodin et al. used laser to process MoS_2 reservoirs into amorphous carbon matrix and found that the composite coating exhibited low friction coefficient of 0.15 in humid air [12]. However, the process is complicated. A simpler technique by co-sputtering MoS_2 and carbon targets was used to fabricate MoS_2-C composite lubricant coatings. Using a r.f. magnetron sputtering method, Pimentel et al. deposited Mo-S-C coatings and tested the tribological properties in humid air. It was concluded that the composite coatings with the C content of 55% showed the lowest friction [13]. Although previous works have made breakthroughs in fabricating MoS_2-C composite lubricant coatings and gained a low friction coefficient in humid environment, the hardness of the Mo-S-C coatings was too low (approx. 0.7–4 GPa) to maintain better wear resistance, which limited applications of these coatings on rougher substrates [14]. Meanwhile, considering different deposition conditions, the effects of C content on the structures and mechanical properties need further discussion. In addition, the low adhesion between steel substrate and the composite will limit the application of MoS_2-C coatings.

To improve the adhesion of the coatings, fabricating interlayer such as Ti or Si layer by magnetron sputtering is a feasible method. High power impulse magnetron sputtering (HIPIMS) is a magnetron

* Corresponding authors.
E-mail addresses: kepl@nimte.ac.cn (P. Ke), yshzou75@gmail.com (Y. Zou).

http://dx.doi.org/10.1016/j.apsusc.2015.01.057
0169-4332/

sputtering method developed in recent years [15], which exerts a pulsed and high power on targets [16]. HIPIMS could provide denser Ti interlayer than traditional magnetron deposition, due to the high sputtering particle ionization rate which is 2–3 orders of magnitude higher than that of conventional magnetron sputtering [17–19].

In this study, MoS_2-C coatings with various C contents were deposited by direct current magnetron sputtering using MoS_2 and C composite target and Ti interlayers were prepared by HIPIMS. Microstructure, mechanical and tribological properties of the coatings were investigated and analyzed. Results show that the friction coefficient is lower than 0.1 and the hardness of the composite coatings is up to 10.8 ± 0.3 GPa.

2. Experimental details

2.1. Preparation of the MoS_2-C coatings

MoS_2-C coatings were fabricated by direct current magnetron sputtering (DCMS) technique. The sputtering material was a composite target, where small MoS_2 plates were stuck to a graphite target (380 mm × 140 mm × 7 mm). The Ti interlayer was deposited by HIPIMS using a Ti target. Details of the deposition system were described elsewhere [15]. All substrate including Si p (100) and mirror-finished high speed steel (HSS) were cleaned ultrasonically in acetone for 15 min and then dried in air. Before deposition, the base pressure in the vacuum chamber was pumped down to less than 3×10^{-5} Torr, and the substrates were precleaned by argon plasma for 20 min. During deposition, the working pressure was kept at about 2.0×10^{-3} Torr, and the Ar gas flow was kept at 20 sccm. The bias voltage on substrates was −200 V. The Ti interlayer (approx. 200 nm) was first deposited. The impulse frequency was 100 Hz and the impulse width was 200 μs. The pulse voltage was 750 V and direct current of Ti target was 1.0 A. Direct current of DCMS was set as 1.0 A for MoS_2-C deposition. The carbon concentration in the coatings was controlled by changing MoS_2 plates stuck to the target.

2.2. Characterization of the MoS_2-C coatings

A surface profilometer (Alpha-Step IQ) employing a step formed by a shadow mask was used to measure the thickness of as-deposited coatings. X-ray photoelectron spectroscopy (XPS, Axis ultraDLD) using Al Kα radiation with photo energy of 160 eV and radio frequency glow discharge optical emission spectrometry (RF-GD-OES, GDA 750HP) was applied to measure the film composition. Before the measurement, the surface of samples was etched by an Ar^+ ion beam of 2 kV for 30 s. Raman spectroscopy (RENISHAW) with a 532 nm Ar^+ laser was used to evaluate the information of bonding structure. High-resolution transmission electron microscopy (HRTEM, FEI Tecnai F20) was used to analyze the microstructure of the deposited coatings in cross-section. X-ray diffraction (XRD, Bruker AXS D8) measurements were also used to characterize the phase structure of the coatings.

The nano-indentation system (MTS NANO G200) was used to measure the hardness and elastic modulus of the coatings. A CSM scratch tester with a diamond indenter (200 μm tip radius) was applied to study the adhesion of the coatings. During scratching, the normal load increased from 1 N to 70 N and the scratch length was 3 mm at a sliding speed of 3 mm/min. The tribological behavior was tested on a ball-on-plate tribometer (Center for Tribology UMT-3) at room temperature with the humidity of 50% under dry sliding condition. GCr15 steel balls (hardness-HCR60) with a diameter of 6 mm were used as sliding counterparts. All the friction tests were performed under a load of 5 N with a sliding speed at 50 mm/s, the length of wear tracks was 5 mm and the reciprocating frequency was 5 Hz. The total sliding time was 3600 s. After tests, the wear track profiles were measured by the surface profilometer. And the wear rates were evaluated as volume per sliding distance per load [13].

3. Results and discussion

3.1. Structure and chemical composition

Table 1 shows the composition and thickness of the coatings. Before the measurement, Ar^+ erosion is applied to remove the contamination of the surface. Carbon concentration rises with the increasing number of MoS_2 plates. The S/Mo ratios fluctuate in the range 1.0–1.1. Due to the fact that S being sputtered out of the surface more easily than Mo, Ar^+ erosion would cause content deviation from the stoichiometry in the target [20]. In addition, the reaction between MoS_2 and residual atmosphere (particularly H_2 and O_2) would also reduce S content. Thus, actual S/Mo ratios are higher than those calculated values and close to the level where MoS_2 coating could maintain its lubricating character. The result of GD-OES analysis shows that the S/Mo ratio of the MoS_2-C coating (73.1 at.% C) is approximately 1.5 which is also higher than the XPS result. The sputtering yield of MoS_2 is much stronger than carbon under the same deposition condition, therefore the thickness of coatings varied linearly [21], as shown in Table 1.

The chemical bonds of the MoS_2-C coatings with different carbon contents are characterized by XPS spectra as shown in Fig. 1. In order to further analyze the chemical forms, the C 1s, S 2p and Mo 3d spectrum of the coating with C content of 40.9% is fitted by Guassian-Lorentian function. In the S 2p and Mo 3d spectrum, the intensity decreases obviously with carbon content. Fig. 1(a) shows the C 1s XPS spectra of the composite coatings with different C contents. The C 1s spectrum is fitted into three components. Two of them represent the C—C bond (285.4 eV) and C=C bond (284.6 eV) and a shoulder at approximately 283.6 eV corresponds to molybdenum carbide [22–24]. Fig. 1(b) shows the S 2p XPS spectra of the coatings with different carbon contents, which were fitted into four components, representing the MoS_2 structure (162.3 eV and 163.4 eV) and MoS (162.8 eV and 161.6 eV), respectively [15,26]. In Fig. 1(c), Peaks representing Mo^{4+} in MoS_2 (229.3 eV and 232.4 eV) and MoS (228.5 eV and 231.6 eV) structure are also found. The Mo 3d spectrum of all samples show a small shoulder at approximately 226.1 eV represented as the S 2s peak [27]. The Mo—C bond is also confirmed in the Mo 3d spectra at 228.2 eV and 231.3 eV, which tallies with the analysis on the C 1s spectrum [13,23]. The high ionization rate during deposition contributes to the existence of molybdenum carbide. Besides, with increasing carbon content, the peak intensity of C—C bond decreases, which indicates the addition of MoS_2 induces the formation of sp^3 bonds.

The Raman spectra provide a further insight into the structure of the as-deposited coatings. The spectra shown in Fig. 2(a) can be divided into three pieces, which denote MoS_2 (250–500 cm^{-1}), MoO_3 (750–1000 cm^{-1}) and C (1000–1700 cm^{-1}), respectively [13,20]. There are two major peaks (approx. at 370 and 410 cm^{-1}) corresponding to MoS_2. The comparatively sharp peaks of MoS_2 in the as-deposited films can be attributed to the thermal crystallization by its high laser energy during Raman tests [25], since the sharp peaks will disappear when using a lower laser energy. Peaks corresponding to MoO_3 at 820 and 960 cm^{-1} are observed. Raman spectra of the carbon can be deconvolved into two peaks, the G peak centered at around 1560 cm^{-1} and the D peak centered at around 1390 cm^{-1}. The G peak is due to the bond stretching of sp^2 atoms in both rings and chains, and the D peaks due to the breathing modes of sp^2 atoms only in rings. Changes of I_D/I_G and the G peak position can indirectly reflect the content change of sp^2 and sp^3 carbon

Table 1
Composition and thickness of the MoS_2-C coatings.

Number of MoS_2 plates	Chemical composition (at.%)				S/Mo ratio	Thickness of the films (μm)
	O	C	Mo	S		
2	4.1	73.1	10.8	12.0	1.1	0.7
4	3.9	59.7	17.6	18.8	1.1	1.0
6	4.2	47.7	24.0	24.1	1.0	1.2
8	5.7	40.9	25.5	27.9	1.1	1.3

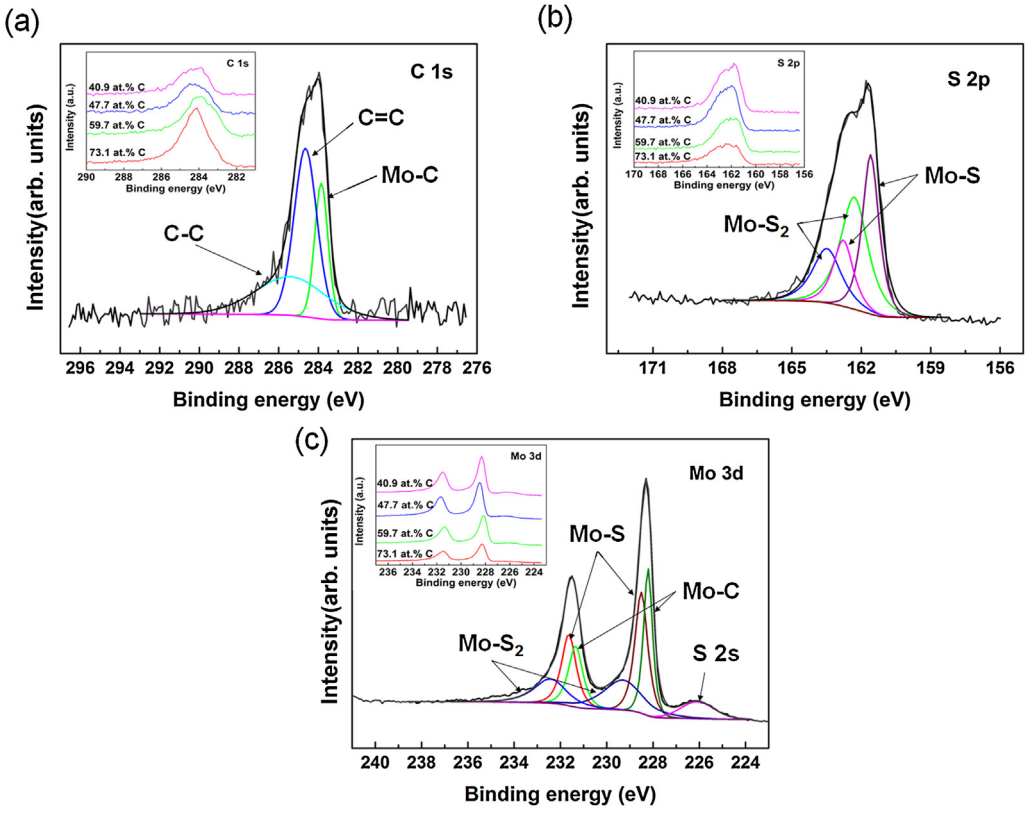

Fig. 1. XPS spectra of MoS_2-C coatings with different C contents, and decomposition of the C 1s (a), S 2p (b) and Mo 3d (c) spectral region of the selected coating (40.9 at.% C).

atoms [28,29]. Fig. 2(b) shows that I_D/I_G ratio increased from 3.93 to 4.69, while G-peak position shifted little, indicating that sp^3 carbon atoms decreased with increasing C content in the MoS_2-C composite coatings. In addition, the intensity of MoS_2 peaks increased with increasing pieces of MoS_2 plates, which coincides with XPS results.

The cross-sectional HRTEM micrographs of the composite coatings (40.9 at.% C) are shown in Fig. 3. The MoS_2-C coatings are divided into three regions, Ti layer, Ti-MoS_2-C layer, and MoS_2-C layer, as shown in Fig. 4(a). Fig. 4(b) demonstrates that nanocrystalline or particulate of MoS_2 are not found in the MoS_2-C composite coatings, which is different from previous works [20,30]. The corresponding selected area electron diffraction (SAED) shows the board and diffuses halo diffraction, which is the typical amorphous feature. Those results illustrate that by sputtering the MoS_2

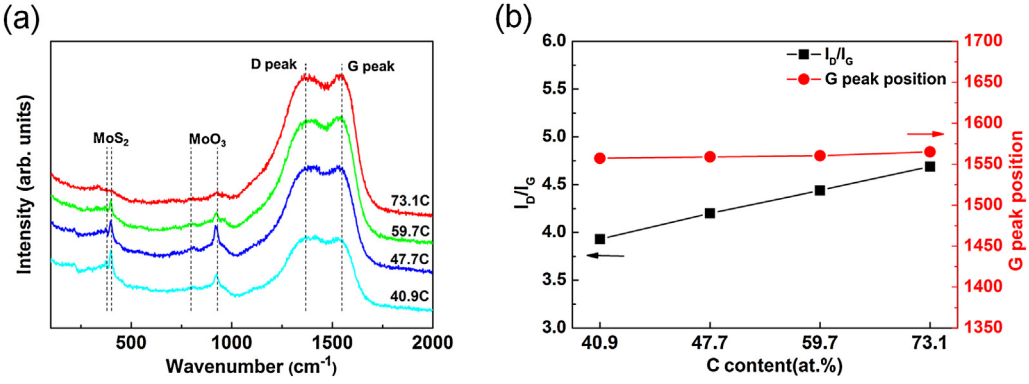

Fig. 2. (a) Raman spectra ofMoS_2-C coatings, and (b) the corresponding I_D/I_G ratio and G-peak position of the composite coatings with different C contents.

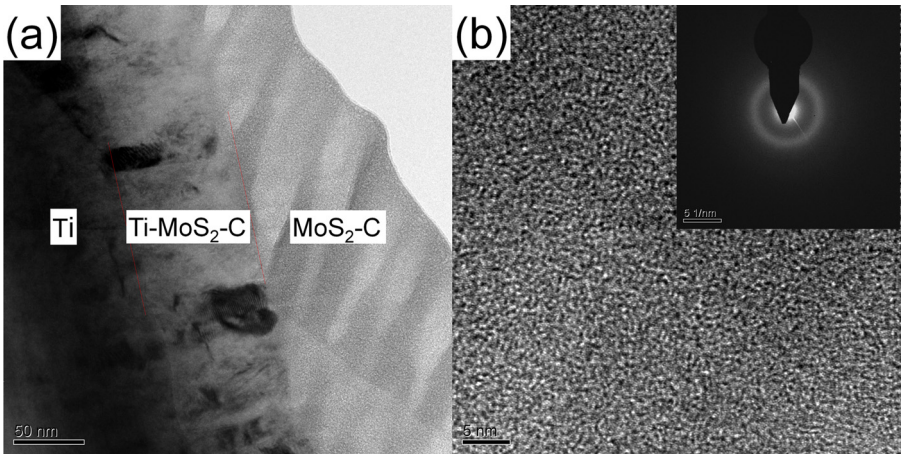

Fig. 3. (a) Cross-sectional HRTEM micrographs of the MoS_2-C coatings with 40.9 at.% C, and (b) HRTEM micrograph and the corresponding SAED of the MoS_2-C layer.

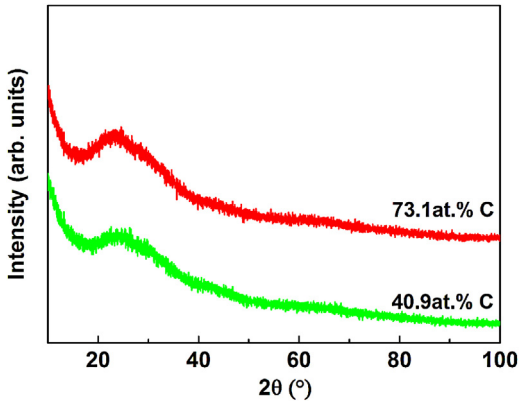

Fig. 4. XRD spectra of MoS_2-C coatings without Ti interlayer. As Ti peak of the interlayer is strong, the MoS_2-C layer was deposited on the optical glass without Ti layer.

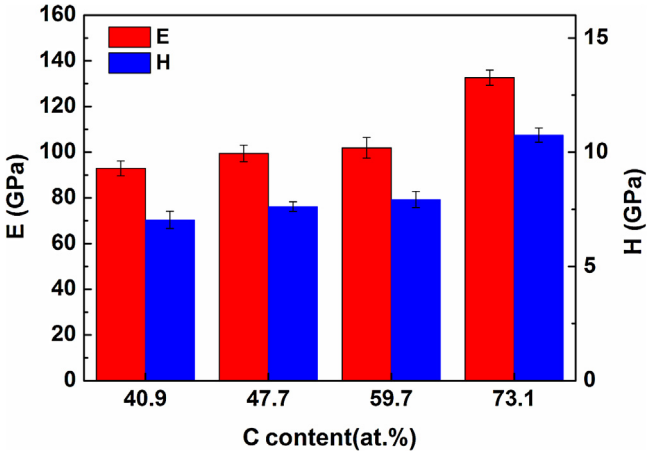

Fig. 5. The hardness (H) and elastic modulus (E) of the MoS_2-C coatings.

and carbon composite target to fabricate MoS_2-C coatings, the MoS_2 are uniformly distributed and dissolved in the DLC structure. The XRD spectra of MoS_2-C coatings without Ti interlayer deposited on the optical glass are shown in Fig. 4 and the spectra confirmed that the MoS_2-C coatings are in the state of typical amorphous structure, which is in agreement with the results of the HRTEM.

3.2. Mechanical characterization

Fig. 5 shows the hardness and elastic modulus of the MoS_2-C coatings. It can be seen that, the hardness of the MoS_2-C coatings varies from 7.0 to 10.8 GPa, which is much higher than that reported in previous works [13]. Several factors may contribute to the high hardness. Compared with the amorphous MoS_2-C coatings, theMoS_2 platelets inserted in the carbon matrix could slip easily and decrease the hardness of the Mo-S-C coatings. Meanwhile, the composited carbon provides a hard matrix. The results also show that the hardness and elastic modulus increase with increasing C content in the composite coatings. Generally, the sp^3 carbon matrix affects the mechanical properties of DLC coatings. According to Raman results, as the C concentration increases, the bonding ratio of sp^3/sp^2 decreases and the relative content of sp^2 atoms increase. Nevertheless, the hardness of the coatings does not decrease with the content of sp^3 atoms. Thus, the reduction of the coating hardness may be owing to the doped MoS_2 content. Doping MoS_2 would destroy the continuity of carbon network and increase the plasticity. Although molybdenum carbide is found by XPS analysis, the presence of hard phase doesn't become the major factor for changes of the hardness [13].

Fig. 6 shows the critical loads of the coatings without interlayer, with Ti interlayer by DCMS and HIPIMS. The results reveal that Ti interlayers prepared by HIPIMS could provide better adhesion properties, and the critical load reaches 56 N. The higher critical load may result from the bombardment of more high-energy Ti particle produced by HIPIMS, resulting in densification and cohesion of coatings.

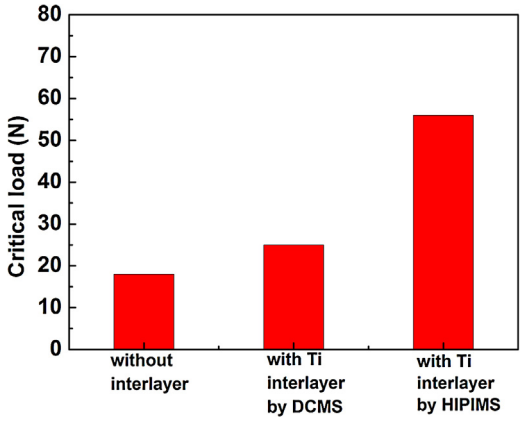

Fig. 6. Critical load of MoS_2-C coatings with Ti interlayers deposited by: without interlayer, DCMS and HIPIMS.

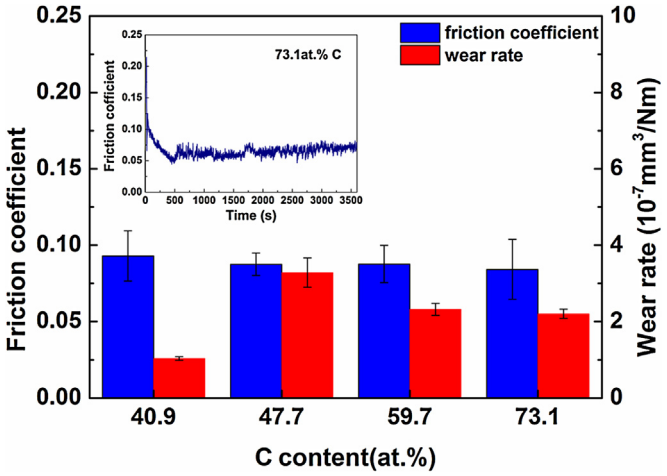

Fig. 7. Average friction coefficient of the composite coatings with different C contents in 50% RH air.

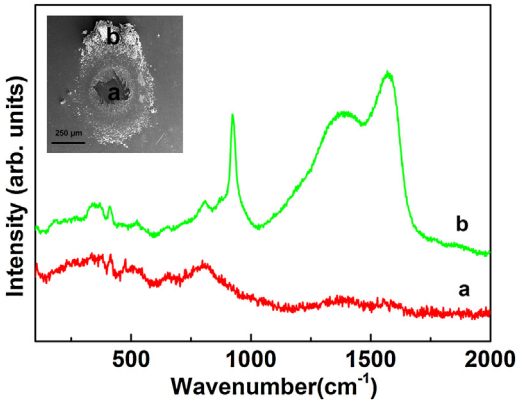

Fig. 8. Raman spectra taken from different parts of the ball after friction test.

3.3. Tribological behavior

Fig. 7 reveals the average friction coefficients and wear rate (under the relative humidity of 50%) as a function of carbon contents and the friction curve of the composite film (73.1 at.% C). It shows that the MoS_2-C coatings exhibit a steady and low coefficient of friction (less than 0.1) against GCr15 steel ball. As the carbon content increases, the coefficient decreases slightly and the coatings wear rate were in the order level of 10^{-7} $mm^3/N\,m$, which is lower than other works [13]. Among these samples, the coatings with carbon content at 40.9 at.% presented the best wear resistance.

Fig. 8 shows the Raman spectra taken from two positions of the counterpart ball after tests with the MoS_2-C films (73.1 at.% C). It can be seen that the transfer film is formed on the ball. Meanwhile, Distinct MoS_2 peaks (approximately 370 and 410 cm^{-1}) found in both spectra acquired in positions (a) and (b) appear sharper than the as-deposited film (Fig. 2), which meant amorphous MoS_2 crystallized during sliding. MoS_2 crystalline in the transfer films can serve as lubricant.

It can be seen that the MoS_2-C composite exhibits low friction and high wear resistance. The TEM and XRD results shows that amorphous MoS_2 is dispersed into dense amorphous carbon matrix which reduces infiltrate of H_2O and O_2 and protects MoS_2 from oxidation. Meanwhile, the amorphous structure also provides MoS_2-C coatings with high hardness and improves endurance in sliding process. In summary, the MoS_2-C coatings will be a good candidate for the tribological application.

4. Conclusion

MoS_2-C coatings with different carbon contents were deposited by direct current magnetron and high power impulse magnetron sputtering. By increasing the number of MoS_2 plates bonded to the carbon targets, carbon content of the coatings changed from 40.9 to 73.1 at.%. XPS results showed that Mo—C bond was found in the composite coatings. The structure of the MoS_2-C coatings exhibited amorphous, which increased the hardness of coatings and further improved the wear resistance of the MoS_2-C coatings. Ti interlayer fabricated by HIPIMS provided a strong bond between MoS_2-C layer and HSS, which benefited from the high ionization rate of HIPIMS. Additionally, despite of the amorphous MoS_2-C layers, the coatings exhibited a low friction coefficient (less than 0.1). The composite structure, which protected MoS_2 from oxidation and improves mechanical properties of the coatings, was thought to account for the excellent friction performance.

Acknowledgements

This research was supported by the National Natural Science Foundation of China (51375475) and the State Key Project of Fundamental Research of China (2013CB632302).

References

[1] T. Polcar, A. Cavaleiro, Self-adaptive low friction coatings based on transition metal dichalcogenides, Thin Solid Films 519 (2011) 4037–4044.
[2] J. Moser, F. Levy, F. Bussy, Composition and growth mode of mosx sputtered films, J. Vac. Sci. Technol. A 12 (1994) 494–500.
[3] C. Donnet, A. Erdemir, Solid lubricant coatings: recent developments and future trends, Tribol. Lett. 17 (2004) 389–397.
[4] P.D. Fleischauer, J.R. Lince, A comparison of oxidation and oxygen substitution in MoS_2 solid film lubricants, Tribol. Int. 32 (1999) 627–636.
[5] N.M. Renevier, J. Hamphire, V.C. Fox, J. Witts, T. Allen, D.G. Teer, Advantages of using self-lubricating, hard, wear-resistant MoS_2-based coatings, Surf. Coat. Technol. 142 (2001) 67–77.
[6] X.Z. Ding, X.T. Zeng, X.Y. He, Z. Chen, Tribological properties of Cr- and Ti-doped MoS_2 composite coatings under different humidity atmosphere, Surf. Coat. Technol. 205 (2010) 224–231.
[7] F. Bülbül, İ. Efeoğlu, MoS_2-Ti composite films having (002) orientation and low Ti content, Crystallogr. Rep. 55 (2010) 1177–1182.
[8] S.M. Aouadi, Y. Paudel, B. Luster, S. Stadler, P. Kohli, C. Muratore, C. Hager, A.A. Voevodin, Adaptive Mo_2N/MoS_2/Ag tribological nanocomposite coatings for aerospace applications, Tribol. Lett. 29 (2008) 95–103.
[9] D.G. Teer, J. Hampshire, V. Fox, V. Bellido-Gonzalez, The tribological properties of MoS_2/metal composite coatings deposited by closed field magnetron sputtering, Surf. Coat. Technol. 94–5 (1997) 572–577.
[10] A. Nossa, A. Cavaleiro, Mechanical behaviour of W–S–N and W–S–C sputtered coatings deposited with a Ti interlayer, Surf. Coat. Technol. 163–164 (2003) 552–560.
[11] H. Niakan, C. Zhang, L. Yang, Q. Yang, J.A. Szpunar, Structure and properties of DLC–MoS_2 thin films synthesized by BTIBD method, J. Phys. Chem. Solids 75 (2014) 1289–1294.
[12] A.A. Voevodin, J. Bultman, J.S. Zabinski, Investigation into three-dimensional laser processing of tribological coatings, Surf. Coat. Technol. 107 (1998) 12–19.
[13] J.V. Pimentel, T. Polcar, A. Cavaleiro, Structural, mechanical and tribological properties of Mo-S-C solid lubricant coating, Surf. Coat. Technol. 205 (2011) 3274–3279.
[14] T. Polcar, F. Gustavsson, T. Thersleff, S. Jacobson, A. Cavaleiro, Complex frictional analysis of self-lubricant W-S-C/Cr coating, Faraday Discuss. 156 (2012) 383.
[15] X. Qin, P. Ke, A. Wang, K.H. Kim, Microstructure, mechanical and tribological behaviors of MoS_2-Ti composite coatings deposited by a hybrid HIPIMS method, Surf, Coat. Technol. 228 (2013) 275–281.
[16] M. Huang, X. Zhang, P. Ke, A. Wang, Graphite-like carbon films by high power impulse magnetron sputtering, Appl. Surf. Sci. 283 (2013) 321–326.
[17] J. In, S. Seo, H. Chang, A novel pulsing method for the enhancement of the deposition rate in high power pulsed magnetron sputtering, Surf. Coat. Technol. 202 (2008) 5298–5301.
[18] K. Sarakinos, J. Alami, S. Konstantinidis, High power pulsed magnetron sputtering: a review on scientific and engineering state of the art, Surf. Coat. Technol. 204 (2010) 1661–1684.
[19] A. Anders, High power impulse magnetron sputtering and related discharges: scalable plasma sources for plasma-based ion implantation and deposition, Surf. Coat. Technol. 204 (2010) 2864–2868.
[20] Y. Wu, H. Li, L. Ji, Y. Ye, J. Chen, H. Zhou, Preparation and properties of MoS_2/a-C films for space tribology, J. Phys. D Appl. Phys. 46 (2013).

[21] Y.X. Wu, H.X. Li, L. Ji, L. Liu, Y.P. Ye, J.M. Chen, H.D. Zhou, Structure, mechanical, and tribological properties of MoS_2/a-C:H composite films, Tribol. Lett. 52 (2013) 371–380.
[22] L.L. Wang, R.Y. Wang, S.J. Yan, R. Zhang, B. Yang, Z.D. Zhang, Z.H. Huang, D.J. Fu, Structure and properties of Mo-containing diamond-like carbon films produced by ion source assisted cathodic arc ion-plating, Appl. Surf. Sci. 286 (2013) 109–114.
[23] L. Ji, H. Li, F. Zhao, W. Quan, J. Chen, H. Zhou, Atomic oxygen resistant behaviors of Mo/diamond-like carbon nanocomposite lubricating films, Appl. Surf. Sci. 255 (2009) 4180–4184.
[24] P. Mérel, Direct evaluation of the sp^3 content in diamond-like-carbon films by XPS, Appl. Surf. Sci. 136 (1998) 105–110.
[25] P.P. Lottici, D. Bersani, M. Braghini, A. Montenero, Raman scattering characterization of gel-derived titania glass, J. Mater. Sci. 28 (1993) 177–183.
[26] J.C. Bernède, About the preferential sputtering of chalcogen from transition metal dichalcogenide compounds and the determination of compound stoichiometry from XPS peak positions, Appl. Surf. Sci. 171 (2001) 15–20.
[27] M.A. Baker, R. Gilmore, C. Lenardi, W. Gissler, XPS investigation of preferential sputtering of S from MoS_2 and determination of MoS_x stoichiometry from Mo and S peak positions, Appl. Surf. Sci. 150 (1999) 255–262.
[28] P.K. Chu, L. Li, Characterization of amorphous and nanocrystalline carbon films, Mater. Chem. Phys. 96 (2006) 253–277.
[29] A.C. Ferrari, J. Robertson, Interpretation of Raman spectra of disordered and amorphous carbon, Phys. Rev. B 61 (2000) 14095–14107.
[30] T. Takeno, S. Abe, K. Adachi, H. Miki, T. Takagi, Deposition and structural analyses of molybdenum-disulfide (MoS_2)–amorphous hydrogenated carbon (a-C:H) composite coatings, Diam. Relat. Mater. 19 (2010) 548–552.